# Conformational Fine-Tuning of Pore-Forming Peptide Potency and Selectivity

Aram J. Krauson, O. Morgan Hall, Taylor Fuselier, Charles G. Starr, W. Berkeley Kauffman,
and William C. Wimley*

Department of Biochemistry and Molecular Biology, Tulane University School of Medicine, New Orleans, Louisiana 70112, United States

ABSTRACT: To better understand the sequence−structure−function relationships that control the activity and selectivity of membrane-permeabilizing peptides, we screened a peptide library, based on the archetypal pore-former melittin, for *loss-of-function* variants. This was accomplished by assaying library members for failure to cause leakage of entrapped contents from synthetic lipid vesicles at a peptide-to-lipid ratio of 1:20, 10-fold higher than the concentration at which melittin efficiently permeabilizes the same vesicles. Surprisingly, about one-third of the library members are inactive under these conditions. In the negative peptides, two changes of hydrophobic residues to glycine were especially abundant. We show that loss-of-function activity can be completely recapitulated by a single-residue change of the leucine at position 16 to glycine. Unlike the potently cytolytic melittin, the loss-of-function peptides, including the single-site variant, are essentially inactive against phosphatidylcholine vesicles and multiple types of eukaryotic cells. Loss of function is shown to result from a shift in the binding−folding equilibrium away from the active, bound, α-helical state toward the inactive, unbound, random-coil state. Accordingly, the addition of anionic lipids to synthetic lipid vesicles restored binding, α-helical secondary structure, and potent activity of the "negative" peptides. While nontoxic to mammalian cells, the single-site variant has potent bactericidal activity, consistent with the anionic nature of bacterial membranes. The results show that conformational fine-tuning of helical pore-forming peptides is a powerful way to modulate their activity and selectivity.
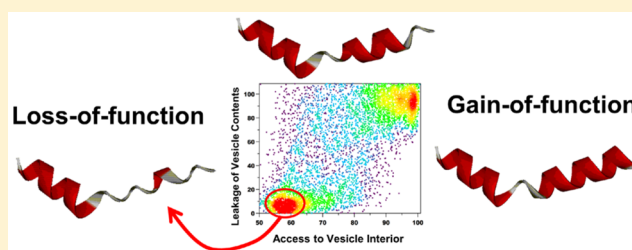
INTRODUCTION

Membrane-permeabilizing peptides have many potential applications, including their use as antibacterial, antifungal, and antiviral compounds,[1−5] as anticancer agents,[6,7] as drug delivery enhancers,[8] and as biosensors.[9,10] However, to realize their full potential, we must be able to rationally engineer or modulate their activity and membrane selectivity, objectives which are currently not possible because the mechanism of such peptides cannot yet be described with specific molecular models. In fact, because many membrane-permeabilizing peptides act non-specifically through their interfacial activity,[11−13] they may have multiple overlapping mechanisms, and it may never be possible to define their activity in explicit molecular terms.

The best-studied example of a potentially useful membrane-permeabilizing peptide is melittin, the archetypal, amphipathic, α-helical cytolytic peptide from the venom of the European honeybee (*Apis mellifera*). Melittin has been closely studied for decades in both synthetic and biological systems.[14−16] Many attempts have been made to harness and control the membrane-permeabilizing activity of melittin for translational applications. For example, researchers have used melittin as a foundation for antimicrobial peptides, with the goal of decreasing its lytic activity against eukaryotic membranes while maintaining its activity against bacterial membranes. In

one such strategy, a diastereomeric version of melittin, with multiple D-amino acids, could not fold into an amphipathic helix, and was thus no longer lytic against mammalian cells but still had good antimicrobial activity.[13] In another case, a chimeric antimicrobial peptide with improved properties was engineered by combining a portion of melittin and a portion of cecropin A, an antibacterial peptide from insects.[17−19] Other researchers have tried to increase or control the activity of melittin so that it could be used as a synthetic ion channel, biosensor, or anticancer agent.[6,7] For example, template-assembled melittin tetramers have potent pore-forming activity.[20,21] Melittin molecules incorporated into targeted nanoparticles (called "nanobees"[22]) have anticancer activity[6,7] and also inhibit the HIV virus, while leaving eukaryotic cells unharmed.[23] Yet, despite the significant amount of research, we cannot currently make quantitative predictions about changes in the activity of melittin upon alterations to its sequence. Thus, neither melittin nor other membrane-active peptides can be rationally engineered.

In the literature, novel variants with useful functions are usually found by trial and error. In our recent work, we have embraced the spirit of trial and error, along with rational design,

to find novel membrane active peptides using synthetic molecular evolution (i.e., iterative rational library design and high-throughput screening).[24] One of our screens[25] led to the discovery of gain-of-function variants of melittin that are equilibrium pore-formers with significantly increased potency, compared to melittin. Although we did not specifically screen for macromolecular poration in the gain-of-function screen, we have shown that the most active gain-of-function variant, MelP5,[25] is unique among known pore-forming peptides in that it releases macromolecules from lipid vesicles at low concentration.[26]

Melittin in membranes has two independent helical segments, separated by the helix-breaking glycine at position 12 and proline at position 14.[27,28] We showed that two single-amino-acid changes to the 26-residue sequence of melittin, Thr 10 to Ala (T10A) and Lys 23 to Ala (K23A), are sufficient, and may be necessary, to drive the observed increases in pore-forming potency.[25] Both of these changes enable the gain-of-function sequences to have more ideal amphipathic helices. The T10A variation improves helical propensity and amphipathicity in the N-terminal helix, while the K23A variation improves helicity and amphipathicity in the C-terminal helix by enabling the extension of the amphipathic helical segment into the cationic C-terminal tail of melittin.

Here we continue our effort toward learning how to "fine-tune" the activity of pore-forming peptides, such as melittin, by screening for loss-of-function variants using the same melittin-based library that was used to find the gain-of-function variants. The difference is that in the loss-of-function assay we screened for *inactive* sequences at a peptide-to-lipid ratio (P:L) of 1:20, while in the gain-of-function assay we screened for potent activity at P:L = 1:1000. For comparison, melittin becomes active at around P:L = 1:200 in this system. We show that both gain- and loss-of-function sequences are dominated by single-amino-acid changes that alter the coupled equilibria of membrane binding, α-helix formation, and membrane permeabilization.

RESULTS AND DISCUSSION

Two-Step Screen. We previously described the two-step screen that we have used to select for potent, equilibrium pore-forming peptides.[24,25,29] First, we measure permeabilization of lipid vesicles by the net release of entrapped terbium citrate after peptide addition. Second, we test for the continued presence of "pores" at equilibrium (>8 h after peptide addition) by measuring the degree to which a membrane-impermeant, polar compound, dithionite, can quench lipid-linked nitrobenzoxadiazole (NBD) fluorophores inside lipid vesicles. Equilibrium permeabilization, which is rare at low peptide concentration,[24,25,29] allows dithionite inside the vesicles at equilibrium, and 100% of NBD moieties are quenched. After transient permeabilization,[11] which is a common mechanism, membranes are no longer permeable at equilibrium. In this case only the external lipid-linked NBD (~55%) will be quenched by dithionite. This screen has successfully been used in two different studies to select for distinct classes of potent, gain-of-function pore-forming peptides under stringent conditions of low peptide-to-lipid ratio, P:L = 1:1000.[24,25,29] One of these gain-of-function screens[25] was performed with the same library and the same lipid vesicles that we use here.

Screening for Loss of Function. In order to learn more about the sequence features that modulate the activity of pore-forming peptides, we screened for *loss-of-function* sequences

using the same melittin-based library and the same lipid vesicles, made from 90% 1-palmitoyl-2-oleoyl-*sn*-glycero-3-phosphocholine (POPC) and 10% 1-palmitoyl-2-oleoyl-*sn*-glycero-3-phosphoglycerol (POPG), that were used in the gain-of-function screen. We screened ~8000 individual library members at P:L = 1:20, a peptide concentration that is at least 10 times higher than the concentration at which melittin efficiently permeabilizes the same vesicles, and is at least 100 times higher than the concentration at which the best gain-of-function peptide, MelP5, efficiently permeabilizes these vesicles. The library design is shown in Figure 1A. The rationale for the 10 varied residues includes (i) modulation of conformational flexibility, (ii) changes in the angle subtended by the polar face, (iii) disruption of a leucine zipper motif, and (iv) polarity and charge of the C-terminal tail.[25] The 7776 member library
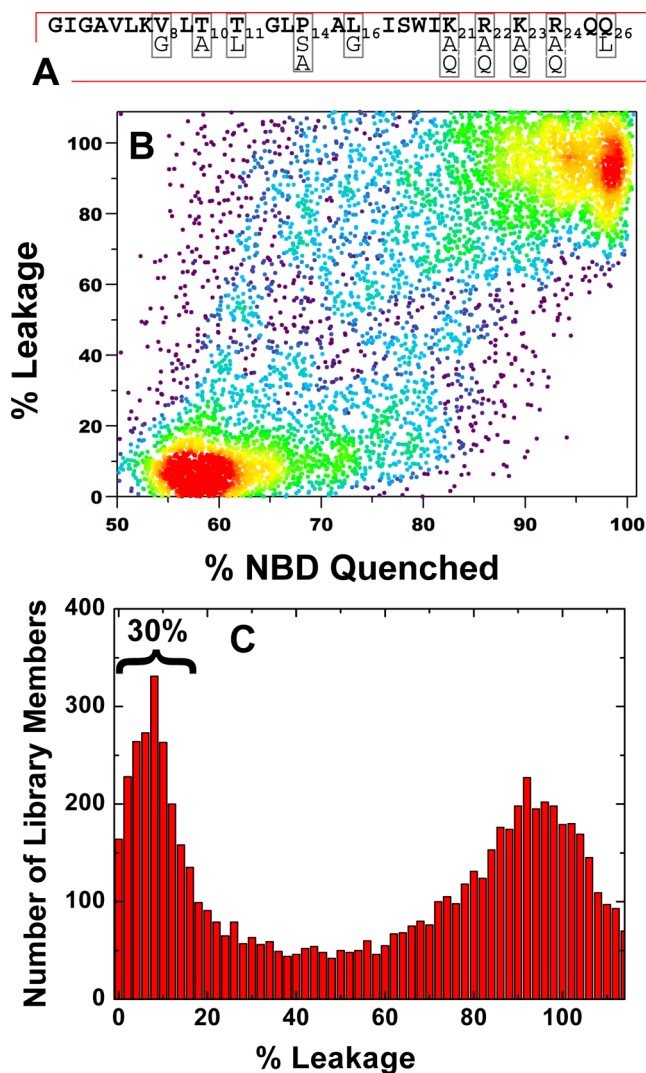

Figure 1. Library and screen. (A) The design of the 7776-member library is based on the sequence of melittin (top line). The boxed and numbered positions were varied using the residues indicated, which also including the native residue. (B) Results of 8000 library members screened at P:L = 1:20 using the two-step screen (see text) against POPC vesicles. Each point represents the results of a single library bead. Point color is determined by local point density in rainbow order, with red representing the highest density. (C) Histogram of leakage activity from the library screen. The % leakage on the *X*-axis is the same measurement that is plotted on the *Y*-axis of panel B.

	1	2	3	4	5	6	7	8	9	10	11	12	13	14	15	16	17	18	19	20	21	22	23	24	25	26
Melittin	G	I	G	A	V	L	K	V	L	T	T	G	L	P	A	L	I	S	W	I	K	R	K	R	Q	Q
Variations								G		A	L			A/S		G					A/Q	A/Q	A/Q	A/Q		L
MelP5	G	I	G	A	V	L	K	V	L	A	T	G	L	P	A	L	I	S	W	I	K	A	A	Q	Q	L
MelN1	G	I	G	A	V	L	K	G	L	T	T	G	L	S	A	L	I	S	W	I	A	Q	Q	Q	Q	L
	G	I	G	A	V	L	K	G	L	A	L	G	L	A	A	G	I	S	W	I	A	Q	Q	R	Q	Q
	G	I	G	A	V	L	K	G	L	A	L	G	L	P	A	G	I	S	W	I	K	Q	Q	Q	Q	L
	G	I	G	A	V	L	K	G	L	A	L	G	L	P	A	G	I	S	W	I	A	?	?	Q	Q	?
	G	I	G	A	V	L	K	V	L	A	T	G	L	A	A	L	I	S	W	I	K	Q	K	R	Q	Q
MelN2	G	I	G	A	V	L	K	G	L	T	L	G	L	A	A	L	I	S	W	I	K	Q	Q	A	Q	Q
	G	I	G	A	V	L	K	V	L	T	T	G	L	P	A	G	I	S	W	I	K	R	A	A	Q	Q
	G	I	G	A	V	L	K	G	L	A	T	G	L	P	A	G	I	S	W	I	K	Q	Q	A	Q	L
	G	I	G	A	V	L	K	V	L	T	L	G	L	P	A	G	I	S	W	I	A	A	Q	A	Q	L
	G	I	G	A	V	L	K	G	L	T	L	G	L	P	A	G	I	S	W	I	Q	Q	K	R	Q	Q
	G	I	G	A	V	L	K	G	L	A	T	G	L	S	A	G	I	S	W	I	Q	A	A	Q	Q	Q
	G	I	G	A	V	L	K	G	L	T	L	G	L	P	A	G	I	S	W	I	A	Q	Q	A	Q	Q
% Conservation																										
Loss of function (this work)								25		50	42			50		25					42	8	17	25		58
Gain of function[25]								78		21	100			100		93					43	43	7	36		50

Figure 2. Sequences of peptides identified in the screen: top line, melittin, from which the library was designed; second line, residue variations in the combinatorial peptide library; and third line, MelP5, the best gain-of-function sequence identified by us in another screen.[25] The loss-of-function sequences were determined by Edman degradation using 12 randomly selected negative library members. Blue columns are varied residues. Red amino acid codes represent changes in residues that were conserved in gain-of-function sequences. Red and green rows highlight two peptides tested for activity. In terms of the changes to glycine at sequence positions Val 8 and Leu 16, MelN1 is atypical, while MelN2 is typical. The bottom two rows show the % conservation of native residue in the loss-of-function screen (this work) and the gain-of-function screen.[25]

explores a narrow sequence space around the parent sequence of melittin.

The scatterplot in Figure 1B shows raw screen results for the individual library members. Inactive peptides are clustered in the lower left and active peptides are clustered in the upper right. Prior to performing the screen, we expected loss-of-function sequences to be rare because most library members are very similar to melittin and MelP5, and were expected to have at least some activity at this very high concentration. The median identity to melittin within the library is 77%. The minimum possible identity is 16/26 residues or 62%. Most library members are more than 80% identical to either melittin or to one of the 10 known gain-of-function variants.[25] Furthermore, our gain-of-function screen showed that the C-terminal tail can vary significantly among active peptides. The scatterplot in Figure 1B and the histogram of leakage in Figure 1C show that our expectation was wrong. There are two specific areas containing an abundant concentration of library members. There is the expected cluster at high activity (>80% leakage, >80% NBD quenching), but also an unexpected cluster with no activity (<20% leakage, <60% NBD quenching). Loss-of-function sequences are surprisingly abundant in the library, with at least one-third of library members having no activity

even at P:L = 1:20. Because the variable sites in the library (Figure 1A) had only two or three possible amino acids, the observed distribution is consistent with the presence of one single-amino-acid change that can abolish activity under these conditions.

We randomly selected 12 loss-of-function library members for sequencing by Edman degradation. We note that up to 1 or 2% of library beads do not release sufficient peptide for detection of activity (unpublished observation). Because the amount of peptide release is not known individually for the 12 negative sequences in Figure 2, it is possible that some are false negatives, due to poor release. Compared to the gain-of-function sequences, there is more overall variability in the loss-of-function sequences. In the identified negatives, the four cationic residues of the C-terminus, overall, were neither conserved nor changed to uncharged residues more often than expected by chance ($p < 0.05$). Similarly, other varied residues did not show statistically significant preferences in the negatives, presumably because the sample size is small. However, two residues, Val 8 and Leu 16, are simultaneously (i) mostly conserved in the gain-of-function sequences, and (ii) mostly changed to glycine in the loss-of-function sequences (Figure 2). Because Val 8-to-Gly was also found in some

validated gain-of-function sequences,[25] we expect that its contribution to activity is complex. Here we focus on Leu 16, which was almost completely conserved in the gain of function variants, and was almost completely changed to glycine the loss-of-function variants.

In a preliminary test, we synthesized a representative loss-of-function sequence, MelN2, which has the commonly observed Val 8-to-Gly and Leu 16-to-Gly variations, along with some changes at the C-terminus. This sequence is highlighted green in Figure 2. We also synthesized an atypical sequence, MelN1, highlighted in red, which we suspected was a false negative because it lacked both the common changes. Indeed, we found that MelN1 has pore-forming potency that is similar to the parent peptide melittin (not shown). It was studied no further in this work. On the other hand, as we describe in detail next, MelN2 is a true negative. Despite having 77% identity to melittin and 81% identity to MelP5, MelN2 has almost no membrane-permeabilizing activity in POPC vesicles, even at very high concentration. Finally, to test the contribution of the Leu 16-to-Gly change, we synthesized a synthetic peptide, Mel L16G, which has the parent sequence of melittin except for that single-amino-acid variation. We show below that the single change recapitulates all of the loss-of-function activity.

Vesicle Permeabilization. In all of the experiments that follow, we study four closely related 26-residue, melittin-derived peptides in parallel: the parent sequence, **melittin**; the gain-of-function peptide, **MelP5**; the observed loss-of-function sequence, **MelN2**; and the engineered loss-of-function sequence, **Mel L16G**. All sequences are shown in Figure 2. The observed gain-of-function and loss-of-function peptides, MelP5 and MelN2, both have charges of +3 and differ by only five residues: an 81% identity. Melittin and Mel L16G have charges of +6 and differ by one residue. They are 96% identical. With these four peptides, which are all highly soluble in aqueous buffers, we measured peptide-induced leakage of the dye ANTS and its quencher DPX from zwitterionic POPC vesicles as a function of peptide concentration. Results are shown in Figure 3. Melittin and MelP5 behave as reported elsewhere.[30] We define the potency using the 50% leakage-inducing concentration, or LIC_{50}, the peptide-to-lipid ratio at which 50% leakage occurs. Melittin permeabilizes POPC vesicles, with LIC_{50} of 1:200, while MelP5, which is more potent, has LIC_{50} of 1:1000. The behavior of the two loss-of-function sequences are extraordinary; they have almost no effect on bilayer permeability except at extremely high concentrations. Their LIC_{50} values are ≫1:10 (Figure 3A,C). Remarkably, even the single-residue change, L16G, completely recapitulates the loss of function of MelN2, observed in the screen. We conclude that the L16G variation is likely responsible for the surprising abundance of loss-of-function variants observed in the screen, because 50% of library members have this variation (Figure 1).

For membrane-permeabilizing amphipathic α-helices, exemplified by melittin, membrane binding, secondary structure formation, and membrane permeabilization are all tightly coupled. Melittin binds to bilayer surfaces, folds into two independent, amphipathic α-helical segments that are connected by a flexible segment around the glycine at position 12 an the proline at position 14, inserting partially into the membrane interface as a bent helix in an orientation generally parallel to the membrane surface.[31] Insertion is driven by the hydrophobic faces of the two helical segments. The flexibility around Pro 14 is critical for the permeabilizing activity of
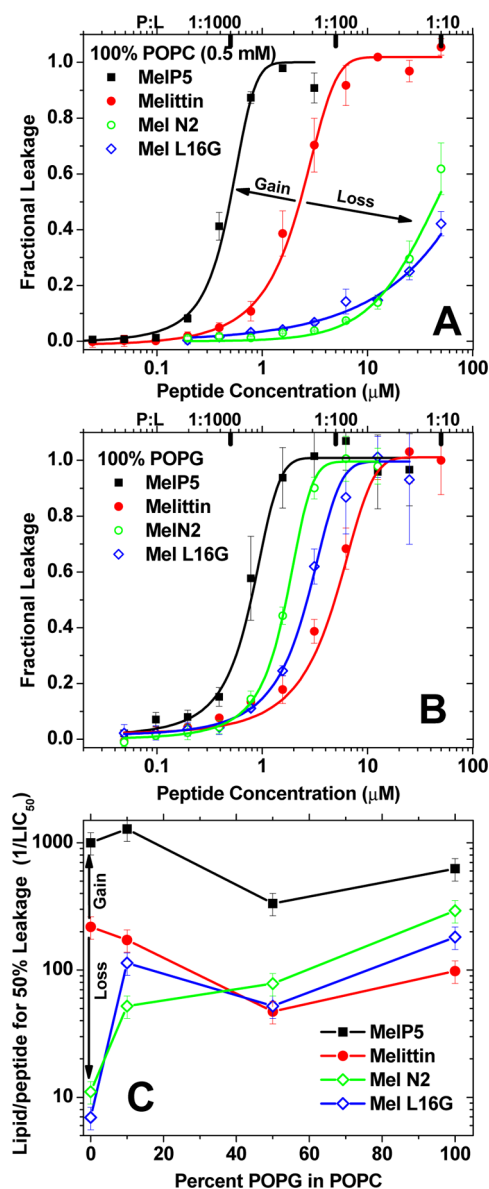

Figure 3. Vesicle leakage. (A) Leakage of ANTS/DPX from 0.5 mM POPC vesicles by peptide serially diluted from 50 to 0.024 μM. Each point is the average of at least three independent measurements. Error bars are SEM. The gain- and loss-of-function derivatives of melittin (red) are indicated. The colors and symbols in panel A are used throughout this work. (B) Leakage of ANTS/DPX from 0.5 mM POPG vesicles by serially diluted peptide. Each point is the average of at least three independent measurements. Error bars are SEM. (C) Summary of leakage experiments. The midpoint of each leakage curve, expressed as $1/LIC_{50}$, is plotted against POPG content. The gain- and loss-of-function derivatives of melittin (red) are indicated as in panel A.

melittin.[27,32] In support of this, we showed that Pro 14 is 100% conserved, and thus essential, in the gain-of-function variants, including MelP5.[25]

There are several (non-mutually exclusive) hypotheses to explain the loss of function caused by L16G in these melittin-like peptides. First, by taking away a large bulky side chain and adding a small flexible one, the amino acid change at L16 could prevent the peptide from attaining the required, active conformation needed to permeabilize membranes, even when bound to membranes. Second, the flexibility of glycine could
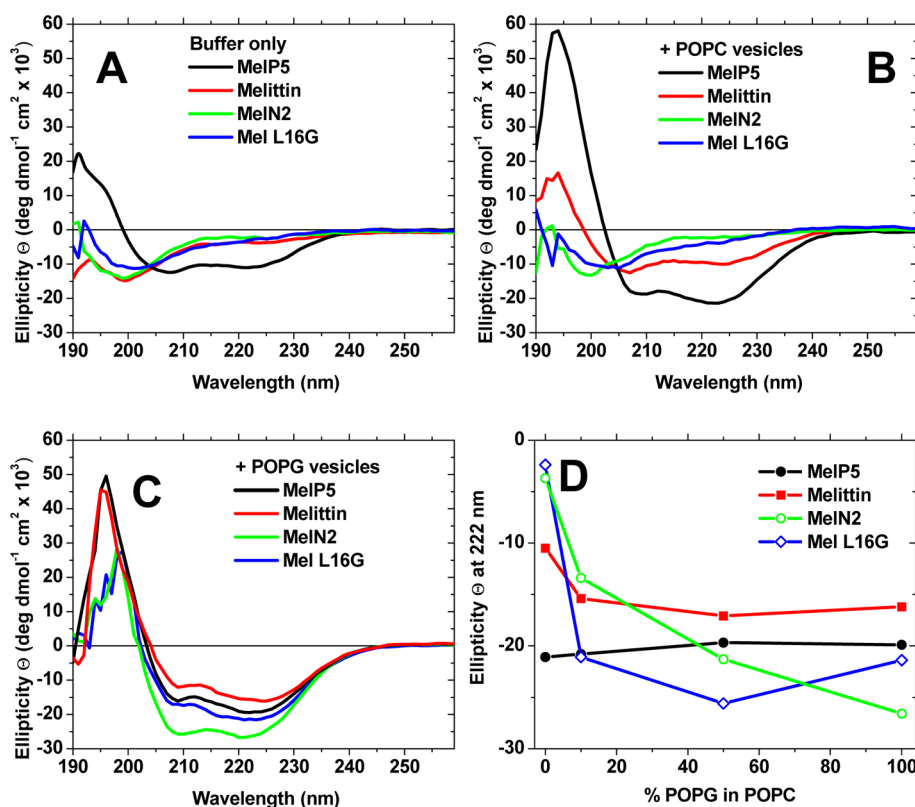
Figure 4. Secondary structure of the peptides. (A) Circular dichroism spectra of 50 μM peptide solutions in buffer. (B) CD spectra of the same solutions shown in panel A, after the addition of 2 mM POPC vesicles. (C) Circular dichroism spectra of the four peptides with 2 mM POPG vesicles. (D) Summary of CD spectra is shown by plotting mean residue ellipticity of the α-helix minimum at 222 nm. The value expected for 100% α-helix is about −33 400.

enable the peptide to attain an inactive conformation not normally accessible. Third, L16G breaks up the ideal "leucine zipper"-like motif comprising residues L6, L9, L13, L16, and I20, which has been suggested to be important for the structure and activity of melittin.[33,34] Lastly, the change of a hydrophobic, helix-favoring Leu residue to a less hydrophobic, helix-breaking Gly could shift the coupled equilibria between binding, structure and function away from the bound, helical and active state of the parent peptide toward an unbound, non-helical, inactive state.

To test these hypotheses, we take advantage of the fact that these peptides are cationic, with charges of +6 for melittin and Mel L16G, and +3 for MelP5 and MelN2. Thus, the strength of their membrane binding can be independently modulated with anionic lipids. We tested all four peptides for leakage activity in lipid vesicles containing anionic POPG at 10%, 50%, and 100%. In 100% POPG, where binding is the strongest, the activity of MelP5 decreases slightly, to LIC_{50} = 1:670. Melittin's activity decreases also to LIC_{50} = 1:100, as reported previously.[30] Most remarkably, both of the so-called "loss-of-function" sequences are highly active in POPG bilayers. In fact, they are both more active than melittin in 100% POPG, with LIC_{50} = 1:190 for Mel L16G and 1:300 for MelN2. MelN2 and Mel L16G are similarly active in 50% POPG, and even 10% POPG bilayers, as shown by the summary data in Figure 3C. Although many cationic, membrane-active peptides are more active in anionic bilayers than zwitterionic bilayers, it is unusual to find a change in behavior as dramatic as we observed here, especially for a peptide like MelN2 that only has a charge of +3.

We note that the *loss-of-function* sequences were identified using vesicles with 10% anionic POPG in a high ionic strength buffer, 300 mM NaCl (see below). However, these same "negatives" are active in 10% POPG vesicles in the assays that we discuss here, probably because the lower ionic strength used here (40 mM versus 300 mM NaCl, previously) promotes binding to 10% POPG vesicles by electrostatic interactions, discussed below.

Secondary Structure. The fact that we were able to observe potent permeabilization by MelN2 and Mel L16G in vesicles containing POPG showed that the loss-of-function sequences are not conformationally prohibited from permeabilizing bilayers. Therefore, it seems likely that the negative peptides do not permeabilize POPC bilayers because they do not bind to, or fold into a helix in, POPC bilayers. To test this idea, we measured circular dichroism spectra for all four peptides in buffer and in the presence of vesicles made of POPC or mixtures of POPC and POPG. The results are shown in Figure 4. In buffer, melittin, MelN2, and Mel L16G are random coils, as indicated by their minima at 200 nm. MelP5 has partial helical structure in buffer, in agreement with its greater amphipathicity. In the presence of POPC vesicles, the CD spectra agree closely with the permeabilization activity in Figure 3. MelP5 is highly helical and highly active. Melittin is also helical and active, but less so. The negative sequences, MelN2 and Mel L16G, are almost completely random coil and are inactive. Because membrane binding and α-helical secondary structure are tightly coupled in all melittin-like peptides, our observation of random coil secondary structure for MelN2 and Mel L16G shows that they do not bind

measurably to POPC bilayers under these conditions. This explains their lack of activity in leakage assays in POPC vesicles.

In contrast, in vesicles made from 100% POPG, all four peptides are highly α-helical (Figure 4C). Helicity again mirrors leakage behavior. In Figure 4D we show the ellipticity at the helix minimum at 222 nm for all four peptides as a function of POPG content. Even the addition of only 10% POPG, shifts the secondary structure of MelN2 and Mel L16G from random coil into highly active, helical state (Figure 4D). Because the effect of 10% charged lipids on binding is expected to be small,[35] especially on MelN2 which has a charge of +3, these results suggest that the negative peptides, while inactive in POPC, are poised near their active state. Only in this case, would a small change in propensity for membrane binding drive a cooperative transition from a mostly inactive, unbound, random coil state to an active, membrane-bound, α-helical state. This idea is further supported by the observation that the activity of MelN2 and Mel L16G against vesicles with 10% POPG is strongly affected by ionic strength; it is zero in the screen (at 300 mM NaCl) but high in the leakage assays (in 40 mM NaCl) where electrostatic membrane binding will be stronger.

Cytolytic Activity. The external face of a eukaryotic cell plasma membrane is rich in zwitterionic lipids, PC and sphingomyelin, and uncharged cholesterol, presenting a membrane surface that contains only small amounts of anionic lipids.[36] For this reason, eukaryotic membranes are susceptible to membrane-permeabilizing peptides, such as melittin, that interact mainly via hydrophobic interactions, but are less susceptible to cationic, membrane-permeabilizing peptides, such as antimicrobial peptides, that interact with membranes mainly via electrostatic interactions. We showed above that the Mel negative peptides differ from melittin and MelP5 in that the negatives require at least a small amount of anionic lipids in order to bind, fold, and permeabilize membranes. Here, we test the ability of these four peptides to permeabilize eukaryotic cell plasma membranes to explore the correlation between activity in synthetic and biological membranes.

To answer this question we first measured the peptide-induced lysis of human erythrocytes (Figure 5A). Performed in PBS, this experiment measures the propensity of the peptide to enable large scale water permeation across the plasma membrane, which leads to osmotic rupture of the cells.[16] The concentration required for 50% effect (EC_{50}) by melittin is 1.2 μM, reflecting its actual biological activity as an indiscriminate cytolysin. Interestingly, the "gain-of-function" peptide MelP5 is slightly less active in erythrocyte membranes, with EC_{50} = 3.0 μM. The negatives, MelN2 and Mel L16G are almost completely inactive against erythrocytes, with extrapolated EC_{50} values that are greater than 1 mM peptide. Just as in POPC vesicles, even the single-amino-acid L16G variant is orders of magnitude less active against mammalian cell membranes than melittin.

We also measured cytotoxicity against three types of nucleated cells: Chinese hamster ovary cells (CHO), human ovarian cancer-derived cells (HeLa), and human colon cancer-derived cells (HCT116) (Figure 5B). Although there is some variability, the behavior of the four peptides is very similar to that observed in erythrocytes. Melittin is the most active, with EC_{50} = 1−2 μM. MelP5 has EC_{50} = 2−3 μM (Figure 5B). Against HeLa and HCT116 cells the negative peptides, MelN2 and Mel L16G, showed no activity at all up to 50 μM (EC_{50} > 500 μM). Against CHO cells, they caused low-level toxicity
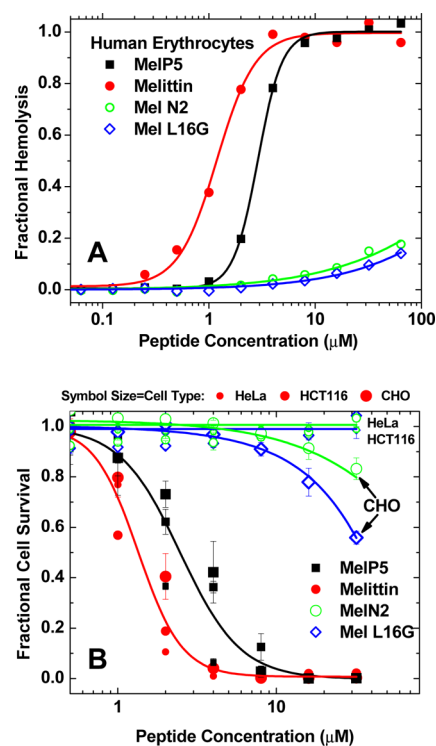

Figure 5. Lysis of eukaryotic cells. (A) Hemolysis was measured by incubating serially diluted peptide with washed human erythrocytes, at 2×10^8 cells/mL, for 1 h at 37 °C, followed by centrifugation of the cells and measurement of released hemoglobin in the supernate. (B) Toxicity of peptides toward nucleated cells, measured with Alamar blue. Adherent cell monolayers at ~80% confluency were treated with serially diluted peptide for 24 h. Alamar blue was added and incubated for 4 h. The fluorescence intensity of reduced Alamar blue (indicating live cells) was measured in a plate reader.

with extrapolated EC_{50} values of 100−300 μM. Taken together, the cytolysis/cytotoxicity measurements recapitulate the observations made in 100% POPC vesicles; the two negative peptides, including the single-amino-acid variant, are 2−3 orders of magnitude less active as membrane-permeabilizing peptides than melittin and MelP5.

It has been reported that cancer-derived cells are more susceptible to membrane permeabilization by cationic anti-microbial peptides due to the fact that they have dysregulated transmembrane lipid asymmetry and present more anionic lipids on the external face.[37−39] However, the loss-of-function peptides we characterize here show similarly inactivity against immortalized but non-cancer-derived CHO cells, as they do against cancer-derived HeLa and HCT116 cells, suggesting that the activity of AMPs against cancer cells may be more complex than simple electrostatics.

Antimicrobial Activity. Finally, we tested the antimicrobial activity of the four peptides against Gram-negative *Escherichia coli* and Gram-positive *S. aureus* bacteria, using broth dilution assays[40] (Figure 6A). Melittin has excellent activity against both microbes, with minimum sterilizing concentrations (MSC) less than 5 μM. This is consistent with its function as a non-specific membrane lytic peptide. Against *E. coli*, MelP5 has similar activity, yet against *Staphylococcus aureus* MelP5 is inactive (MSC > 40 μM). This is likely because MelP5 is helical in solution (Figure 4A) and may exist as multimers, which cannot readily diffuse through the cell wall of the Gram-positive bacteria, while they can bind to and permeabilize the outer
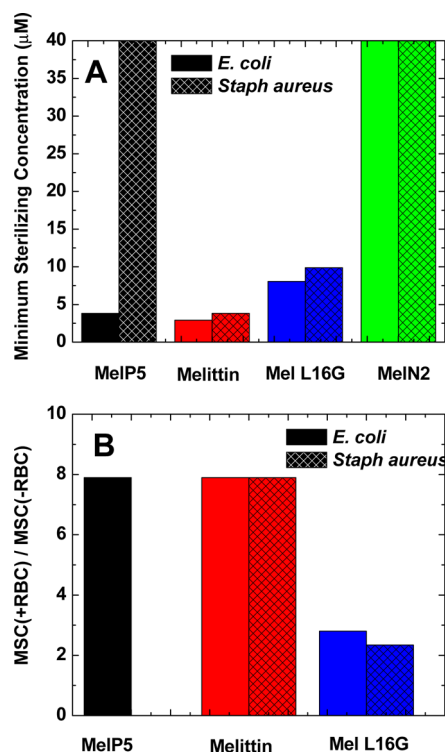
Figure 6. Antibacterial activity. (A) Minimum sterilizing concentrations against *E. coli* and *S. aureus* were determined with standard broth dilution assays[40] averaged over at least three independent experiments. Peptide concentrations were serially diluted from 40 μM; thus, any bars at 40 μM indicate a lack of observed activity. (B) MSC measurements were made using broth dilution in which all steps were done in the presence of 1×10^9 erythrocytes (RBCs) per mL. The *Y*-axis is the ratio of the MSC in the presence of erythrocytes to the MSC in their absence.

membrane of Gram-negative bacteria thereby accessing the inner membrane. Unlike the case for POPC vesicles and eukaryotic cells (Figures 3 and 5), Mel L16G is highly active against both *E. coli* and *S. aureus*. The observed negative, MelN2 is inactive (MSC > 40 μM) against both bacteria. We cannot currently explain why these two peptides behave differently in bacterial membranes, when they are very similar in PC band PG-containing synthetic bilayers. Perhaps the high anionic charge on the bacterial cytoplasmic membranes promotes strong binding of Mel L16G, which has a charge of +6, but that the binding of MelN2 which has a charge of +3, is not sufficient for good activity. In vesicle assays, perhaps the lower charge of MelN2 is compensated by its higher hydrophobicity or amphipathicity when the peptide solution is in direct contact with the membrane, while this is not the case for bacterial cytoplasmic membranes which are only accessed by peptides that pass through the cell wall or outer membrane. While anionic synthetic membranes can mimic bacterial membranes in many ways, this result shows that the correlation is incomplete.

Finally, we combined eukaryotic and prokaryotic cells to indirectly test the relative binding of the peptides. Because Mel L16G is more dependent on membrane charge for binding than melittin and MelP5, we hypothesized that Mel L16G will have a greater preference for the bacterial membrane when both types of cells are present. To test this idea, we measured the degree to which the addition of 1×10^9 human erythrocytes per ml (20% of the concentration in whole blood) reduces antimicrobial

activity (increases MSC value) of the active peptides. The stronger the competitive binding to erythrocytes, the greater the effect on MSC should be. The data in Figure 6B support the hypothesis: while 1×10^9 erythrocytes/mL increased the MSC of melittin and MelP5 by 8-fold, it increased the MSC of L16G by only 2-fold, supporting the idea of much weaker binding of Mel L16G to erythrocytes. This agrees with the low hemolytic activity of Mel L16G. These data suggest that Mel L16G or variants of it could be nontoxic and have reasonable antimicrobial activity in whole blood (5×10^9 erythrocytes/mL) where many antibiotic peptides are somewhat toxic and are inactive due to host cell binding.

Conformational Fine-Tuning. To enable improved rational design of membrane-permeabilizing peptides, here we sought to learn how to better control the activity of melittin by screening a narrowly defined, melittin-based library for loss-of-function sequences. The results show that changing only the natural leucine at position 16 to glycine is sufficient, and may be necessary, to abolish activity against PC vesicles as well as against mammalian cells. Further, we demonstrated that the loss of activity against these membranes is due to a shift in the peptide-membrane equilibrium away from the bound, helical and active state. The peptide conformational equilibrium lies just outside of the conditions at which binding and activity occur in PC vesicles. We refer to this effect as "conformational fine-tuning". The potential for practical applications of these peptides are shown by the fact that Mel L16G is a broad spectrum antibiotic which causes little or no hemolysis or cytotoxicity against mammalian cells. A dramatic change in the potential usefulness of melittin is achieved by a single-amino-acid change.

Ladokhin and White and others[41–43] have described the thermodynamics of partitioning and folding of melittin and other amphipathic peptides in POPC bilayers as a combination of interfacial hydrophobicity (net −0.1 kcal/mol for melittin) and about −0.4 kcal/mol per residue favoring the partial folding of the membrane-bound peptide. The latter contribution is dominated by the hydrophobic moment of the helical segments. The result, for melittin, is a sequence that binds well to POPC, with $\Delta G_x = -7.8$ kcal/mol, and which has about 60–70% helix content. The gain-of-function peptide MelP5 is more hydrophobic (net −2.9 kcal/mol), more amphipathic, and has a higher helix content in membranes (Figure 4), consistent with its stronger binding (−8.2 kcal/mol).[25]

In this framework, the L16G change is predicted to reduce the hydrophobicity of the variant, relative to melittin, by only 0.6 kcal/mol,[44,45] which is not enough to solely account for the complete loss of binding and activity of Mel L16G in POPC. Conformational effects that reduce helical propensity must also contribute to loss of activity. Because folding of short helices is strongly influenced by end group effects,[46] the conformational effects are likely maximized by placement of the flexible, helix-inhibiting glycine[47] at position 16 near the end of the C-terminal helical segment of melittin in membranes. The conformational effect of L16G on melittin structure and function is opposite to the effect of K23A, one of the most important changes in the gain-of-function sequences. K23A increases helical propensity by enabling the extension of the C-terminal amphipathic helical segment into the cationic C-terminal tail of melittin.

CONCLUSION

We have shown here that changing a single, critical hydrophobic leucine at position 16 to a flexible glycine in the bee venom peptide, melittin, dramatically changes the selectivity of the peptide for membranes through conformational fine-tuning. Unlike the potent and indiscriminately lytic parent sequence, and its gain-of-function variants, the loss-of-function variant does not strongly bind to or permeabilize synthetic PC bilayers, and is not lytic or toxic against multiple types of eukaryotic cells. Importantly, we show that this effect is accomplished without significantly changing the basic structure−function relationships in the peptide. Instead, it is achieved through conformational fine-tuning of helical propensity, which is directly coupled to binding, structure and activity of amphipathic, α-helical pore formers. In the presence of anionic lipids, perhaps at concentrations higher than those found in eukaryotic cells in culture, the new melittin variants regain potent membrane-permeabilizing activity because increased binding shifts the equilibrium toward the α-helical, membrane-permeabilizing state.

Conformational fine-tuning could have many practical applications. In this work, we show directly that L16G melittin has potentially useful, broad-spectrum antimicrobial activity, with little or no toxicity to host cells. It also has low susceptibility to host cell binding, a problem that may eliminate useful activity of most antimicrobial peptides, in vivo. However, our results also imply other uses for conformationally fine-tuned, membrane-permeabilizing peptides. For example, because cytotoxic activity is directly coupled to binding, one can imagine that the specific binding of an antibody or receptor ligand, labeled with Mel L16G could lead to cell-type specific cytolysis. This would be a useful strategy against cancer cells, pathogens, pathogen-infected cells or other target cells.

MATERIALS AND METHODS

Materials. The peptide library was synthesized using standard FMOC methods as described elsewhere.[48,49] All other peptides were synthesized and purified by Biosynthesis, Inc. Bacteria and nucleated cells were obtained from ATCC and fresh human erythrocytes were obtained from Interstate Blood Bank.

Loss-of-Function Screen. The details of the library design and synthesis and the vesicle-based screen have been described elsewhere.[24,25,29] The library was synthesized as a one-bead one peptide library on large solid phase peptide synthesis beads. Each bead had about 5 μg (~1 nmol) of one sequence tethered to it by a photolabile linker. Library members were released from beads by UV irradiation and then screened against lipid vesicles. Large unilamellar vesicles were made from 89% 1-palmitoyl-2-oleoyl-sn-glycero-3-phosphocholine (POPC) + 10% 1-palmitoyl-2-oleoyl-sn-glycero-3-phosphoglycerol (POPG), plus 1 mol % NBD-labeled-POPE. Terbium chloride (50 mM) and sodium citrate (100 mM) was entrapped inside the vesicles, which was replaced with equiosmolar 300 mM NaCl outside containing 50 μM dipicolinic acid. Leakage is indicated by luminescent complex formation between Tb and DPA.[50] Vesicles were added to wells containing extracted peptide so that P:L = 1:20. After overnight incubation of vesicles and peptide, leakage of terbium was measured using a Biotek Synergy microplate reader. Afterward, freshly prepared dithionite in 1 M K₂PO₄, pH 10 was diluted into each well, and the remaining NBD fluorescence was measured. The negative control in each plate was vesicles with no peptide and the positive control was vesicles in the presence of Triton-X100 detergent.

Vesicle Permeabilization Assays. Large unilamellar vesicles were made by extrusion from POPC and/or POPG. Vesicles contained the dye ANTS (6 mM) and its quencher DPX (12 mM) in 10 mM phosphate buffer as described elsewhere.[51] The external solution contained equiosmolar NaCl at 40 mM in 10 mM phosphate buffer. Peptide serial dilutions were made in lo-bind Eppendorf tubes, followed by addition of 0.5 mM lipid vesicles. After 1 h, samples were added to wells of a 96-well plate and ANTS fluorescence was measured on a Biotek Synergy plate reader. Fractional leakage was calculated using controls that included buffer only (negative), Triton-X-100 (positive), and MelP5 at P:L = 1:100 (positive).

Circular Dichroism. Peptide solutions were prepared in 10 mM NaPO₄ buffer with 40 mM NaCl at 50 μM peptide concentration. CD spectra were collected on a JASCO 810 spectropolarimeter in a 1 mm rectangular quartz cuvette in the absence or presence of 1 or 2 mM lipid vesicles.

Hemolysis. Fresh human red blood cells were obtained from Interstate Blood Bank, Inc., and thoroughly washed in PBS until the supernatant was clear. RBC concentration was determined using a standard hemocytometer. In hemolysis assays serial dilutions of peptide were prepared, followed by the addition of 2×10^8 RBC/mL. After incubation for 1 h at 37 °C the cells were centrifuged and the released hemoglobin was measured by optical absorbance of the heme group (410 nm). Negative control was buffer only (0% lysis), and the positive controls were 20 μM melittin and distilled water (100% lysis).

Cytotoxicity. Cells were seeded in 96-well plates and grown to 80−90% confluency for 1 day prior to addition of serially diluted peptides. After 24 h of incubation with peptides, Alamar blue, which is reduced in live cells to a fluorescent compound, was added and cells were incubated for an additional 4 h. Measurement of fluorescence was done using a Biotek Synergy plate reader. Controls were buffer only (negative) or 25 μM MelP5 (positive).

Antibacterial Assays. Escherichia coli strain ATCC 25922 and Staphylococcus aureus strain ATCC 25923 were used in this study. Overnight cultures were subcultured to log phase (OD_{600} = 0.3−0.6) after which cell counts were determined by measuring the OD_{600} (1.0 = 1.5×10^8 CFU/mL for S. aureus, 5×10^8 CFU/mL for E. coli). Bacteria in minimal media mere added to serially diluted peptides and incubated for 3 h, followed by the addition of full growth media. After overnight incubation, the optical density of the wells read on a plate reader to determine whether they were sterilized (OD < 0.08) or were at stationary phase growth, OD > 0.5. Intermediate values, which were rare, were considered positive for growth. Average minimum sterilizing concentrations were calculated from the lowest peptide concentration that sterilized the bacteria in each serial dilution. Broth dilution assays done in the presence of RBCs were done using two plates, a growth plate (as above) which was used to inoculate a secondary plate that contained sterile media. After overnight growth of the secondary plate, optical densities were read as above.

AUTHOR INFORMATION

Corresponding Author

*wwimley@tulane.edu

Notes

The authors declare no competing financial interest.

ACKNOWLEDGMENTS

REFERENCES

(1) Hancock, R. E.; Sahl, H. G. Nat. Biotechnol. 2006, 24, 1551−1557.

(2) Duggineni, S.; Srivastava, G.; Kundu, B.; Kumar, M.; Chaturvedi, A. K.; Shukla, P. K. Int. J. Antimicrob. Agents 2007, 29, 73−78.

(3) Makovitzki, A.; Avrahami, D.; Shai, Y. Proc. Natl. Acad. Sci. U. S. A. 2006, 103, 15997−16002.

(4) Jenssen, H.; Hamill, P.; Hancock, R. E. Clin. Microbiol. Rev. 2006, 19, 491−511.

(5) Lok, S. M.; Costin, J. M.; Hrobowski, Y. M.; Hoffmann, A. R.; Rowe, D. K.; Kukkaro, P.; Holdaway, H.; Chipman, P.; Fontaine, K. A.; Holbrook, M. R.; Garry, R. F.; Kostyuchenko, V.; Wimley, W. C.; Isern, S.; Rossmann, M. G.; Michael, S. F. *PLoS One* **2012**, *7*, e50995.

(6) Soman, N. R.; Baldwin, S. L.; Hu, G.; Marsh, J. N.; Lanza, G. M.; Heuser, J. E.; Arbeit, J. M.; Wickline, S. A.; Schlesinger, P. H. *J. Clin. Invest.* **2009**, *119*, 2830−2842.

(7) Jo, M.; Park, M. H.; Kollipara, P. S.; An, B. J.; Song, H. S.; Han, S. B.; Kim, J. H.; Song, M. J.; Hong, J. T. *Toxicol. Appl. Pharmacol.* **2012**, *258*, 72−81.

(8) Gerlach, S. L.; Rathinakumar, R.; Chakravarty, G.; Goransson, U.; Wimley, W. C.; Darwin, S. P.; Mondal, D. *Biopolymers* **2010**, *94*, 617−625.

(9) Yin, P.; Burns, C. J.; Osman, P. D.; Cornell, B. A. *Biosens. Bioelectron.* **2003**, *18*, 389−397.

(10) Cornell, B. A.; Braach-Maksvytis, V. L. B.; King, L. G.; Osman, P. D. J.; Raguse, B.; Wieczorek, L.; Pace, R. J. *Nature (London, U. K.)* **1997**, *387*, 580−583.

(11) Wimley, W. C. *ACS Chem. Biol.* **2010**, *5*, 905−917.

(12) Bechinger, B.; Lohner, K. *Biochim. Biophys. Acta, Biomembr.* **2006**, *1758*, 1529−1539.

(13) Shai, Y.; Oren, Z. *Peptides* **2001**, *22*, 1629−1641.

(14) Tosteson, M. T.; Tosteson, D. C. *Biophys. J.* **1981**, *36*, 109−116.

(15) DeGrado, W. F.; Musso, G. F.; Lieber, M.; Kaiser, E. T.; Kézdy, F. J. *Biophys. J.* **1982**, *37*, 329−338.

(16) Dempsey, C. E. *Biochim. Biophys. Acta, Rev. Biomembr.* **1990**, *1031*, 143−161.

(17) Oh, D.; Shin, S. Y.; Kang, J. H.; Hahm, K. S.; Kim, K. L.; Kim, Y. *J. Pept. Res.* **1999**, *53*, 578−589.

(18) Vunnam, S.; Juvvadi, P.; Rotondi, K. S.; Merrifield, R. B. *J. Pept. Res.* **1998**, *51*, 38−44.

(19) Mancheño, J. M.; Oñaderra, M.; Martínez del Pozo, A.; Díaz-Achirica, P.; Andreu, D.; Rivas, L.; Gavilanes, J. G. *Biochemistry* **1996**, *35*, 9892−9899.

(20) Pawlak, M.; Meseth, U.; Dhanapal, B.; Mutter, M.; Vogel, H. *Protein Sci.* **1994**, *3*, 1788−1805.

(21) Grove, A.; Mutter, M.; Rivier, J. E.; Montal, M. *J. Am. Chem. Soc.* **1993**, *115*, 5919−5924.

(22) Pan, H.; Soman, N. R.; Schlesinger, P. H.; Lanza, G. M.; Wickline, S. A. *Wiley. Interdiscip. Rev. Nanomed. Nanobiotechnol.* **2011**, *3*, 318−327.

(23) Hood, J. L.; Jallouk, A. P.; Campbell, N.; Ratner, L.; Wickline, S. A. *Antiviral Ther.* **2013**, *18*, 95−103.

(24) Krauson, A. J.; He, J.; Hoffmann, A. R.; Wimley, A. W.; Wimley, W. C. *ACS Chem. Biol.* **2013**, *8*, 823−831.

(25) Krauson, A. J.; He, J.; Wimley, W. C. *J. Am. Chem. Soc.* **2012**, *134*, 12732−12741.

(26) Wiedman, G.; Fuselier, T.; He, J.; Searson, P. C.; Hristova, K.; Wimley, W. C. *J. Am. Chem. Soc.* **2014**, *136*, 4724−4731.

(27) Dempsey, C. E.; Bazzo, R.; Harvey, T. S.; Syperek, I.; Boheim, G.; Campbell, I. D. *FEBS Lett.* **1991**, *281*, 240−244.

(28) Rex, S. *Biophys. Chem.* **2000**, *85*, 209−228.

(29) Krauson, A. J.; He, J.; Wimley, W. C. *Biochim. Biophys. Acta, Biomembr.* **2012**, *1818*, 1625−1632.

(30) Ladokhin, A. S.; White, S. H. *Biochim. Biophys. Acta, Biomembr.* **2001**, *1514*, 253−260.

(31) Hristova, K.; Dempsey, C. E.; White, S. H. *Biophys. J.* **2001**, *80*, 801−811.

(32) Dempsey, C. E. *Biochemistry* **1992**, *31*, 4705−4712.

(33) Zhu, W. L.; Song, Y. M.; Park, Y.; Park, K. H.; Yang, S. T.; Kim, J. I.; Park, I. S.; Hahm, K. S.; Shin, S. Y. *Biochim. Biophys. Acta, Biomembr.* **2007**, *1768*, 1506−1517.

(34) Asthana, N.; Yadav, S. P.; Ghosh, J. K. *J. Biol. Chem.* **2004**, *279*, 55042−55050.

(35) Ladokhin, A. S.; White, S. H. *J. Mol. Biol.* **2001**, *309*, 543−552.

(36) Daleke, D. L. *Curr. Opin. Hematol.* **2008**, *15*, 191−195.

(37) Riedl, S.; Rinner, B.; Asslaber, M.; Schaider, H.; Walzer, S.; Novak, A.; Lohner, K.; Zweytick, D. *Biochim. Biophys. Acta, Biomembr.* **2011**, *1808*, 2638−2645.

(38) Riedl, S.; Zweytick, D.; Lohner, K. *Chem. Phys. Lipids* **2011**, *164*, 766−781.

(39) Hoskin, D. W.; Ramamoorthy, A. *Biochim. Biophys. Acta, Biomembr.* **2008**, *1778*, 357−375.

(40) Wiegand, I.; Hilpert, K.; Hancock, R. E. *Nat. Protoc.* **2008**, *3*, 163−175.

(41) Ladokhin, A. S.; White, S. H. *J. Mol. Biol.* **1999**, *285*, 1363−1369.

(42) Almeida, P. F.; Ladokhin, A. S.; White, S. H. *Biochim. Biophys. Acta, Biomembr.* **2012**, *1818*, 178−182.

(43) Fernandez-Vidal, M.; Jayasinghe, S.; Ladokhin, A. S.; White, S. H. *J. Mol. Biol.* **2007**, *370*, 459−470.

(44) White, S. H.; Wimley, W. C. *Annu. Rev. Biophys. Biomol. Struct.* **1999**, *28*, 319−365.

(45) Wimley, W. C.; White, S. H. *Nat. Struct. Biol.* **1996**, *3*, 842−848.

(46) Lyu, P. C.; Zhou, H. X.; Jelveh, N.; Wemmer, D. E.; Kellenbach, N. R. *J. Am. Chem. Soc.* **1992**, *114*, 6560−6562.

(47) Padmanabhan, S.; Marqusee, S.; Ridgeway, T.; Laue, T. M.; Baldwin, R. L. *Nature (London, U. K.)* **1990**, *344*, 268−270.

(48) Rausch, J. M.; Marks, J. R.; Wimley, W. C. *Proc. Natl. Acad. Sci. U. S. A.* **2005**, *102*, 10511−10515.

(49) Rathinakumar, R.; Wimley, W. C. *J. Am. Chem. Soc.* **2008**, *130*, 9849−9858.

(50) Wilschut, J.; Papahadjopoulos, D. *Nature (London, U. K.)* **1979**, *281*, 690−692.

(51) Wimley, W. C. *Methods Mol. Biol.* **2015**, *1324*, 89−106.